Tribological behavior and thermal stability of TiC/a-C

Pei, Y.T.; Galvan, D.; De Hosson, J.Th.M.

Published in:
Journal of Vacuum Science & Technology A

DOI:
10.1116/1.2194927

Publication date:
2006

Tribological behavior and thermal stability of TiC/*a*-C:H nanocomposite coatings

Y. T. Pei,[a] D. Galvan, and J. Th. M. De Hosson
Department of Applied Physics, the Netherlands Institute for Metals Research and Materials Science Center, University of Groningen, Nijenborgh 4, 9747 AG Groningen, The Netherlands

(Received 3 May 2005; accepted 13 March 2006; published 23 June 2006)

Advanced TiC/*a*-C:H nanocomposite coatings have been produced via reactive deposition in a closed-field unbalanced magnetron sputtering system (Hauzer HTC-1200). These wear-resistant coatings are targeted for automotive applications where high load-bearing capacity and thermal stability, low friction, and wear resistance are the primary requirements. In this article the tribological behavior of the nanocomposite coatings is scrutinized by means of ball-on-disk tribotests at elevated temperature or after annealing in the temperature range of 150–400 °C. The thermal stability of the coatings in terms of critical temperatures, at which the degradation of wear resistance and friction of the coatings starts, is monitored with depth profiling of oxygen content using Auger spectroscopy in conjunction with detailed examinations of the mechanical properties of the annealed coatings. A striking result is that a coating thermally stable up to 350 °C may fail at much lower temperatures during elevated-temperature tribotests. The origin of failure is attributed to the interfacial delamination due to the discontinuity in mechanical properties between the coatings and substrates at elevated temperatures. It indicates a stringent requirement to optimize the interlayer of advanced tribological coatings developed for high temperature applications. © *2006 American Vacuum Society.* [DOI: 10.1116/1.2194927]

I. INTRODUCTION

Diamondlike carbon (DLC) based nanocomposite coatings have increasingly attracted interest due to their unique combination of chemical-physical properties that maintain the positive characteristics of DLC matrix in conjunction with a nanocrystalline phase, such as stress relaxation, toughening of the amorphous matrix, and improved tribological performance.[1–3] The thermal stability and inherent compressive stresses are two major drawbacks of DLC films, both of which are related to the sp^3 carbon bonding. Much research has been devoted to the study of thermal stability through annealing DLC films in various atmospheres correlating the property degradation with a change in the hybrid structure of sp^2 and sp^3 bonds.[4,5] It has been found that DLC films are thermally unstable beyond 350 °C and that degradation becomes more pronounced above 400 °C via the conversion of sp^3 bonds to sp^2.[6] Such temperatures can be readily reached at hot spots between sliding contacts. However, annealing of DLC films only mimics the thermal attack but ignores the combination with mechanical loading as a major factor for surface fatigue cracking and wear.

In this article, we study the resistance of TiC/*a*-C:H nanocomposite coatings with respect to thermomechanical loading in comparison with thermal stability without loading. A striking result is that a coating thermally stable up to 350 °C in air may fail at much lower temperatures during elevated-temperature tribotests. It indicates a stringent requirement to optimize the interlayer of advanced tribological coatings developed for high temperature applications.

[a]Author to whom correspondence should be addressed; electronic mail: y.pei@rug.nl

II. EXPERIMENT

TiC/*a*-C:H nanocomposite coatings were deposited via closed-field unbalanced reactive magnetron sputtering (CFURMS) in an acetylene/argon atmosphere (C_2H_2/Ar:20%–25%) with a Hauzer HTC-1200 coating system equipped with two Cr targets of purity >99.95% and two Ti targets of purity >99.99% opposing each other and Ar and acetylene gas sources. The set-up of the coating system is nearly the same as the Hauzer HTC-1000 system,[7] except for the larger dimensions of the deposition chamber in the HTC-1200 coating system. The substrates used for each deposition were $\varnothing 30 \times 6$ mm^2 disks of hardened M2 steel and $\varnothing$100 mm Si wafers. Two different interlayers were designed between substrate and coating to improve adhesion, i.e., Cr/CrTi/TiC (Ref. 8) and Ti/TiC, respectively. Flow rate of acetylene gas and substrate bias were the two major deposition parameters varied in the range of 80–125 sccm (sccm denotes standard cubic centimeter per minute) and floating to −150 V, respectively. No intentional substrate heating was applied during the depositions. Nevertheless, the substrate temperature was monitored with a thermocouple and as a consequence of the ion bombardment the substrates reached temperatures in the 180–190 °C range. The deposition was carried on until a coating thickness of about 1.5 μm was reached.

An MTS Nano Indenter XP was employed to measure the hardness and Young's modulus of the coatings with a Berkovich indenter calibrated with fused silica of known hardness and elastic modulus, using the continuous stiffness measurement (CSM) technique. A CSM Revetest scratch tester was used for measuring the interfacial adhesion strength with a diamond stylus of 200 μm radius and 0.01 m/min scratch

TABLE I. Deposition parameters, chemical composition, and properties of nc-TiC/*a*-C:H coatings.

Coating code	Bias (−V)	C_2H_2 (sccm)	Composition[a] (at. %)			Residual stress (MPa)	*H* (GPa)	*E* (GPa)	*H*/*E*	L_{cl} (N)
			C	Ti	O					
100V115	100	115	83.50	15.34	1.16	−641	14.8	124.5	0.119	37
130V115	130	115	83.12	16.02	0.86	−883	17.4	146.9	0.118	36
130V120	130	120	85.42	13.72	0.86	−846	17.4	140.1	0.124	34
60V110	60	110	80.21	16.33	3.46	−352	11.8	99.8	0.118	41
100V110	100	110	81.02	17.84	1.14	−761	15.6	136.6	0.114	38
150V110	150	110	80.30	18.51	1.19	−1595	19.8	168.3	0.118	35
100V80	100	80	66.60	31.75	1.65	−1184	20.0	229.4	0.087	32.5
100V125	100	125	87.19	11.85	0.96	−1154	15.8	128.5	0.123	35

[a]Excluding hydrogen.

speed. The residual stresses of the coatings were measured by monitoring the curvature change of Si wafers after deposition.

All tribotests were performed in air using a CSM high temperature tribometer with a ball-on-disk configuration against ∅6 mm 100Cr6 ball at 0.1–0.3 m/s sliding speed and 5 N normal load. The wear depth/height of the coating sample (disk) and the counterpart ball was *in situ* monitored with a resolution of 0.02 μm by a rotational variable differential transformer (RVDT) sensor during the tribotests, which allowed *in situ* measurements of the thickness of the transfer films on the surface of the counterpart in contact. A confocal microscope was used to capture three-dimensional (3D) images on a wear track for measuring the wear volume. In the ball-on-disk configuration an area of the ball is continuously in contact with the coating, whereas the corresponding areas on the coating sample are only once in contact during a lap. Therefore, the wear rate (W_r) of the coatings is defined as the volume of wear per unit track length, per newton of normal load, and per lap.

The fractured cross sections of the coatings on Si wafer were examined using a field emission scanning electron microscope (Philips FEG-XL30s) and an atomic force microscope (Digital Instruments NanoScope® IIIa) was used to study the surface morphology of the coatings. Glancing incidence x-ray diffraction (GI-XRD) scans were acquired with a Philips PW1877 diffractometer operating with a Cu $K\alpha$ radiation source placed at 1.5° incident angle with respect to the coating surface. The average particle size of TiC nanocrystallites in the coatings was calculated from the full width at half maximum (FWHM) of the TiC (111) and TiC (200) peaks using the Scherrer equation.

Electron probe microanalysis (EPMA) with a Cameca SX-50 wavelength-dispersive (WD) x-ray spectrometer was used to determine the chemical composition of the coatings making use of standards. An acceleration voltage of 5 keV was employed to avoid excitation of x rays from the interlayer area of the coating. Depth profiling of element content with Auger spectroscopy was performed in a dedicated small-spot and ultrahigh vacuum (UHV) scanning electron/scanning Auger microscope derived from a JEOL JAMP 7800F equipped with a field emission gun. Argon ion gun used for sputtering was operated at 3000 eV energy and 7 $\times 10^{-7}$ A current with an on/off time of 10 s each, which yields a sputtering rate of 11 nm/min. The minimum e-beam spot size of about 15 nm was chosen to excite Auger electrons on four sputtered spots of a coating sample for reliable data after each sputtering step. All the depth profiling was done under identical conditions.

III. RESULTS AND DISCUSSIONS

A. Chemistry and microstructure of TiC/*a*-C:H coatings

In our recent article,[1] it was shown that the microstructure of TiC/*a*-C:H nanocomposite coatings is significantly influenced by the substrate bias and flow rate of acetylene gas. The undesired columnar growth can be restrained by increasing substrate bias or carbon content, leading to the formation of a glassy microstructure instead that may exhibit substantial toughness. A superior wear resistance of the nanocomposite coating has been achieved under the condition of low friction and high toughness, both of which require fine TiC nanoparticles (e.g., 2 nm) and a wide matrix separation that must be comparable to the dimensions of the nanoparticles. Accordingly, the appropriate substrate bias ranges between −100 and −150 V, i.e., below the lower limit at which columnar structure occurs and beyond the higher limit where compressive stresses become so strong that the coating may delaminate from the substrate. Excluding hydrogen, the carbon content that is desired is 80–90 at. %, i.e., the composition where the size of TiC nanocrystallites approaches the separation width of amorphous carbon matrix. Based on the observed evolution of nano- and microstructures it is expected that deposition conditions close to the higher limits of substrate bias and carbon content may even yield better TiC/*a*-C:H nanocomposite coatings in terms of optimized nanostructure and properties. Therefore, −130 V substrate bias and 85 at. % carbon content were chosen to complete the parameter matrix of deposition, alongside with a benchmark test at −100 V bias and 115 sccm flow rate of acetylene for the new CFURMS deposition system HCT 1200. In addition, a simplified Ti/TiC layer has been designed as interlayer, in comparison with the previously employed Cr/CrTi/TiC graded interlayer.[8] The deposition parameters, composition, and properties of the new coatings as well as

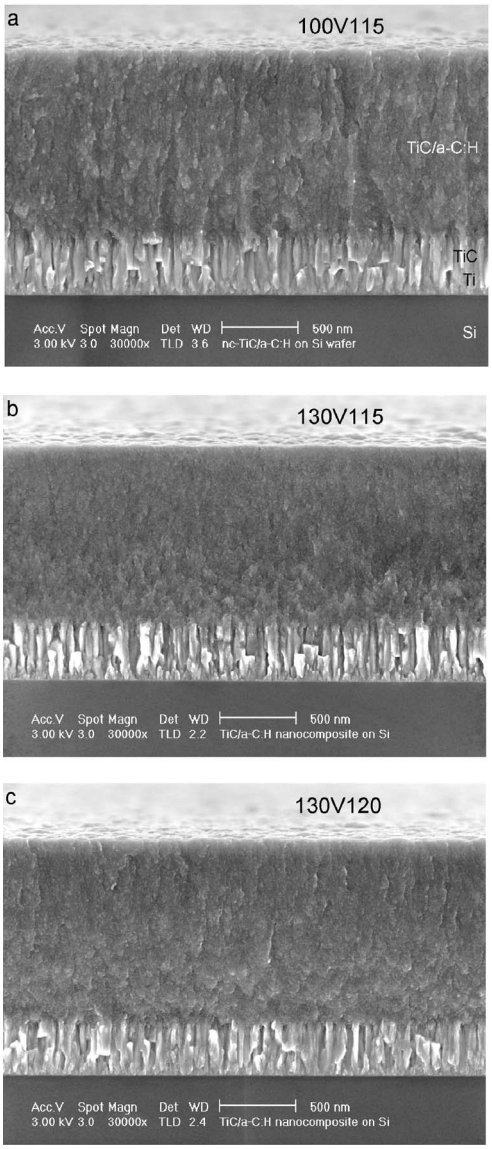

FIG. 1. SEM micrographs of the fractured cross sections of the coatings: (a) 100V115, (b) 130V115, and (c) 130V120.

the previous ones are listed in Table I. The mechanical properties of the new coatings are fully in line with the general trend observed on the previous coatings, that is to say, both the hardness (H) and elastic modulus (E) increase with substrate bias and the H/E ratio increases only with the flow rate of acetylene gas. The residual stress is mainly controlled by the substrate bias, i.e., higher compressive stresses developed at stronger ion bombardment.

Figure 1 shows scanning electron microscopy (SEM) micrographs of the fractured cross sections of the coatings. The coating 100V115 exhibits a very weak columnar microstructure, similar to that observed in 100V110.[1] The reproducibility of the nanocomposite coatings has been confirmed by this benchmark test as well as the microstructures exhibited in the coatings. In contrast, coatings 130V115 and 130V120 are free of a columnar microstructure. Especially, the latter exhibits some tear lips and dimples on the fractured sections, indicating that plastic deformation occurred during fracture of the coatings contributing to fracture toughness. GI-XRD analysis indicates that the mean sizes of TiC nanocrystallites are 2.2 and 2.1 nm in the coatings 130V115 and 130V120, respectively. According to the chemical composition of the coatings measured with EPMA and the mean particle size, the volume fraction of TiC nanocrystallites and the particle mean free path are estimated to be 28.0% and 3.8 nm in the coating 130V115, and 23.4% and 4.6 nm in the coating 130V120, respectively.

The simplified Ti/TiC intermediate layer with a gradual transition from Ti (200 nm) to TiC avoids the cracking tendency inside the Cr/CrTi/TiC intermediate layer, which was often observed in the previous coatings, as seen in Fig. 2(b) of Ref. 1. Scratch tests confirm that the adhesion strength of the coatings to the high-speed steel substrates is comparable to that of the previous coatings employing Cr/CrTi/TiC intermediate layer, with the critical scratching loads (L_{c1}) of 34–37 N against 32.5–41 N, as seen in Table I. Even higher L_{c1} is expected if the thickness of the Ti/TiC intermediate layer reduces from currently about 400 to 200 nm.

TABLE II. Mechanical properties of nc-TiC/a-C:H nanocomposite coatings after annealing in air for 1 h.

		Annealing temperature (°C)						
Coating code	Properties	20[a]	130	200	250	300	350	400
100V115	H (GPa)	14.9				13.2	11.6	6.6
	E (GPa)	124.5				119.4	109.8	102.2
	H/E ratio	0.119				0.111	0.106	0.064
130V115	H (GPa)	17.4	17.3	17.2	17.2	16.7	16.1	
	E (GPa)	146.9	152.1	155.8	147.8	144.3	143.3	
	H/E ratio	0.118	0.114	0.111	0.116	0.116	0.112	
130V120	H (GPa)	17.4				16.3	15.6	
	E (GPa)	140.1				139.2	136.6	
	H/E ratio	0.124				0.117	0.114	
HS steel substrate	HV (GPa)	8.16	8.00	8.06	8.04	8.10	7.90	

[a]As deposited.

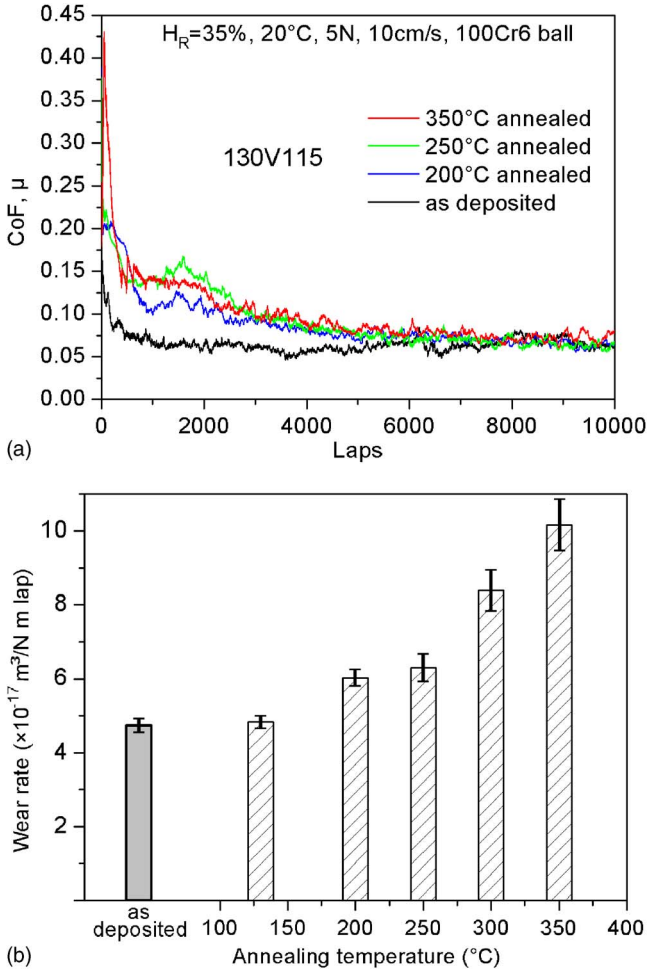

FIG. 2. Influence of annealing temperature on the tribological properties of the coating 130V115: (a) coefficient of friction (CoF) and (b) wear rate, tested at room temperature and 35% relative humidity, 5 N normal load, and 10 cm/s sliding velocity against 100Cr6 ball.

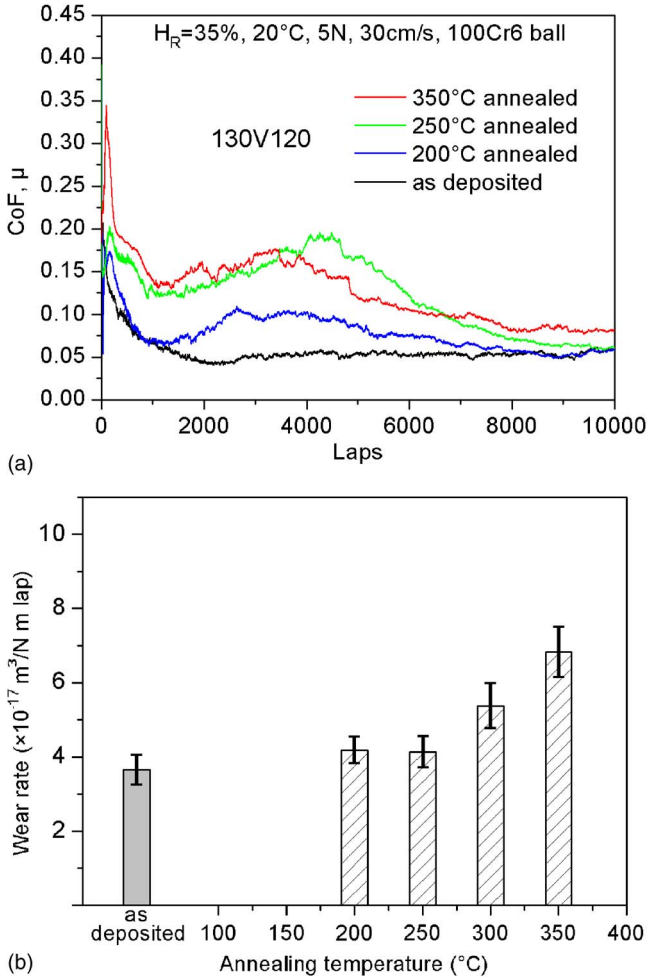

FIG. 3. Influence of annealing temperature on the tribological properties of the coating 130V120: (a) coefficient of friction (CoF) and (b) wear rate, tested at room temperature and 35% relative humidity, 5 N normal load, and 30 cm/s sliding velocity against 100Cr6 ball.

B. Tribological behavior of annealed TiC/*a*-C:H coatings

In order to reveal the thermal resistance of the coatings themselves, hardness and elastic modulus of the coatings have been measured by nanoindentation after annealing for 1 h at various temperatures in air. Table II lists all the mechanical properties of the annealed coatings. It is clear that the coatings are thermally stable up to 250 °C but start to soften at 300 °C. The softening of annealed coatings becomes pronounced above 350 °C. In contrast, bearing steels (e.g., 100Cr6) degrade at the temperature of about 190 °C and the high-speed steel substrates also soften at 350 °C (see Table II). Because engine components are usually made of heat treatable steels or bearing steels, tribological coatings with a thermal resistance above 250 °C are adequate enough for automotive applications.

Figures 2 and 3 demonstrate the tribological performances of the as-deposited and annealed coatings 130V115 and 130V120, respectively, as tested with ball-on-disk dry sliding against ∅6 mm 100Cr6 balls under 5 N normal load. The as-deposited coatings show the typical self-lubricating behavior as observed on the previous coatings.[1] That is to say, the coefficient of friction (CoF) drops from an initially high value of about 0.2 at the beginning of sliding to a low steady-state CoF of about 0.06–0.08 depending on the sliding velocity, after a transition period during which transfer films gradually form on the ball surface in contact. The wear rate of the annealed coatings stays more or less unchanged up to the annealing temperature of 250 °C and significantly increases when annealed at temperatures above 300 °C. In addition, the coatings annealed at higher temperatures exhibit a higher CoF at the onset of a tribotest and need a much longer time to reach the steady-state CoF at a low level. For instance, the peak CoF at the test beginning of 350 °C annealed coatings is twice as high compared to those of the coatings annealed below 250 °C. In other words, annealing at higher temperatures deteriorates the self-lubrication effect. Especially, the coatings with higher carbon content such as 130V120 are more dramatically influenced by annealing [Fig. 3(a)], likely attributed to oxidation of *a*-C:H matrix.

Auger depth profiling of oxygen element in the annealed coatings is shown in Fig. 4 and reveals that oxidation of

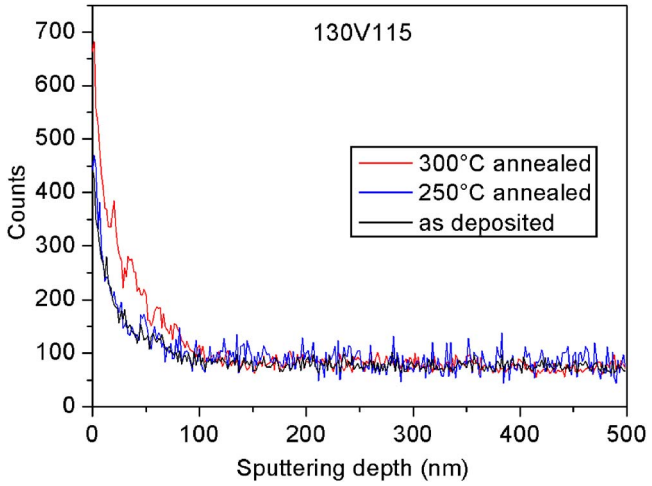

FIG. 4. Auger depth profiling of oxygen element in the coating 130V115 after annealing at different temperatures in comparison with that of the as-deposited coating.

TiC/*a*-C:H coatings for 1 h annealing in air is negligibly small up to annealing temperature of 250 °C. A substantial increase in oxygen content has been detected after annealing at 300 °C. However, the diffusion depth of oxygen is limited to about 100 nm in the annealed coating. Apparently, annealing for a longer time or at higher temperatures will increase further the oxygen content as well as the diffusion depth in the coatings, which may result in heavier degradation of the annealed coatings. This oxidation behavior of a thin surface layer explains the tribotest results that higher CoF at the onset of sliding and longer transition period needed to reach the steady-state CoF are observed on the coatings annealed at higher temperatures. It has been observed before that a high oxygen content in the as-deposited TiC/*a*-C:H coating, such as 0V110 in Ref. 1, leads to a steady-state CoF as high as 0.28 even though the chemical status of oxygen in the coating and the mechanism affecting friction are not clear yet. This remains a subject for further research.

C. Tribological behavior of TiC/*a*-C:H coatings at elevated temperature

Tribotests at elevated temperatures demonstrate that the ultralow friction regime of TiC/*a*-C:H coatings may maintain up to 200 °C, as shown in Fig. 5, where the CoF (~0.01) is even lower than the steady-state CoF of the coatings tested at room temperature. The friction coefficient gradually increases to a medium level of 0.1 as temperature rises above 200 °C. Thereafter, the coatings suddenly fail at about 230 °C with a sliding life less than 3000 laps (revolutions), indicated by a jump of CoF to about 0.6 that is a typical CoF value of dry sliding between metal-to-metal contacts. It indicates that coating delamination is the failure mode, as confirmed by SEM observations in Fig. 6. Although the ramping rate of temperature was different between the two tests due to a different maximum temperature set for

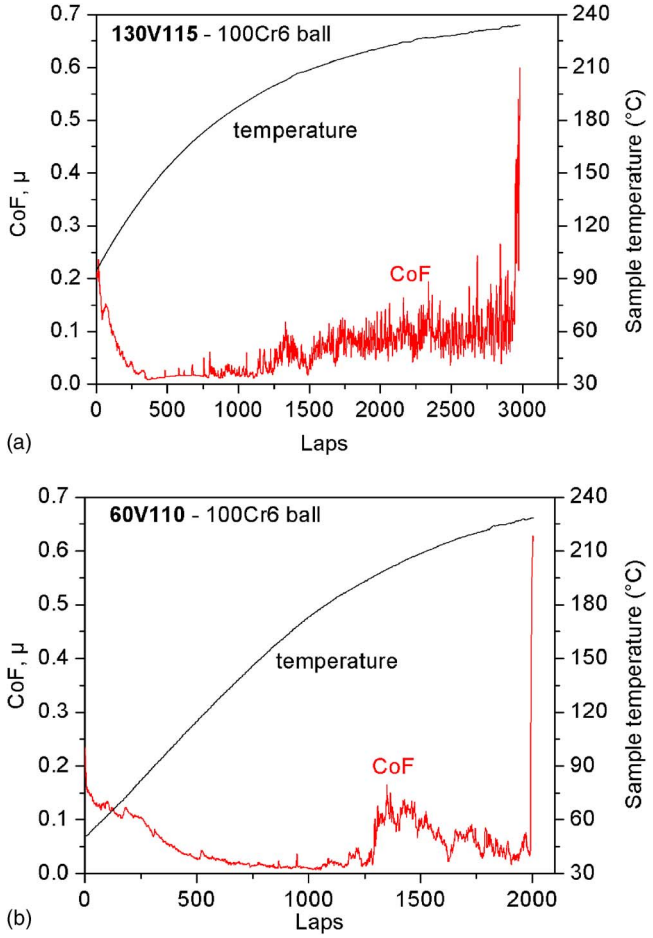

FIG. 5. Elevated temperature tribotesting results of the coatings: (a) 130V115 with Ti/TiC interlayer and (b) 60V110 with Cr/CrTi/TiC interlayer (tested in air of 50% relative humidity, 5 N normal load, and 10 cm/s sliding velocity).

each test, the tribological behavior of the two coatings is rather similar, no matter whether a Ti/TiC or Cr/CrTi/TiC interlayer has been used.

The two different levels of CoF before the coatings abruptly fail deserve several comments. At the early stage of a test the CoF drops to a very low value of about 0.01 as the sample temperature rises rapidly. This phenomenon is attributed to the gradual desorption of water molecules from the sliding surfaces with increasing temperature, whose effect is equivalent to that of decreasing the humidity level of the atmosphere as observed in our recent work.[1] When the sample temperature is above 200 °C, the coating surface oxidizes locally at hot spots on sliding contact where the peak temperature is well above 350 °C. This leads to an increase in oxygen content in the top atomic layers of the coatings and consequently a significant increase in CoF, close to the CoF value of the annealed coatings. In addition, the counterpart 100Cr6 ball and the interlayer start to soften at such high temperatures, which may cause serious problems: the former destroys the transfer films and leads to adhesive wear whereas the latter weakens interface adhesion leading to coating delamination. A possible solution to this problem is

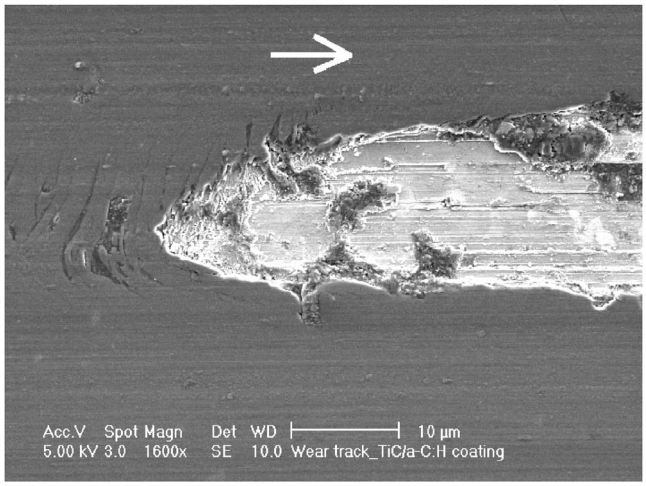

FIG. 6. SEM micrograph of the middle part of the wear track on the coating 130V115 showing a damaged spot where the coating delaminated during the elevated-temperature tribotest. An arrow indicates the moving direction of the ball counterpart.

to introduce a refractory metal interlayer such as W that may stay hard at high temperatures or a high temperature shape-memory interlayer that may exhibit self-healing and superelastic effects.[9]

IV. CONCLUSIONS

The TiC/*a*-C:H nanocomposite coatings designed for wear resistance and low friction have been deposited with closed-field unbalanced magnetron sputtering. The influence of substrate bias and flow rate of acetylene gas on the nano/microstructure and mechanical properties of the coatings is in line with the previously observed results, independent of the CFURMS sputtering systems. TiC/*a*-C:H nanocomposite coatings are thermally stable up to annealing temperatures of 350 °C in air. However, the coatings may fail under elevated temperature tribotesting at 230 °C. The failure mode is coating delamination and is mainly attributed to the soft Ti or Cr interlayer used for enhancement of interfacial adhesion at room temperature. This work indicates a stringent requirement to optimize the interlayer of advanced tribological coatings developed for high temperature applications.

ACKNOWLEDGMENTS

The authors acknowledge financial support from the Netherlands Institute for Metals Research (NIMR) and the Foundation for Fundamental Research on Matter (FOM-Utrecht). Christian Strondl from Hauzer Techno Coating BV (Venlo, the Netherlands) is gratefully acknowledged for his help in the deposition of the coatings. Professor A. Cavaleiro of the Universidade de Coimbra Pinhal de Marrocos, Portugal is thanked for giving support to the EPMA of the composition of the coatings. Gert ten Brink and Paul Huizenga in the authors' group are thanked for their assistance in the Auger depth profiling.

[1]Y. T. Pei, D. Galvan, and J. Th. M. De Hosson, Acta Mater. **53**, 4505 (2005).
[2]T. Zehnder, P. Schwaller, F. Munnik, S. Mikhailov, and J. Patscheider, J. Appl. Phys. **95**, 4327 (2004).
[3]W. J. Meng and B. A. Gillispie, J. Appl. Phys. **84**, 4314 (1998).
[4]R. K. Y. Fu, Y. F. Mei, M. Y. Fu, X. Y. Liu, and P. K. Chu, Diamond Relat. Mater. **14**, 1489 (2005).
[5]W. J. Wu and M. H. Hon, Surf. Coat. Technol. **111**, 134 (1999).
[6]D. R. Tallant, J. E. Parmeter, M. P. Siegal, and R. L. Simpson, Diamond Relat. Mater. **4**, 191 (1995).
[7]C. Strondl, N. M. Carvalho, J. Th. M. De Hosson, and G. J. van der Kolk, Surf. Coat. Technol. **162**, 288 (2003).
[8]D. Galvan, Y. T. Pei, and J. Th. M. De Hosson, Acta Mater. **53**, 4303 (2005).
[9]W. Y. Ni, Y.-T. Cheng, and D. S. Grummon, Appl. Phys. Lett. **80**, 3310 (2002).